

THE 4TH INTERNATIONAL CONFERENCE ON ALUMINUM ALLOYS

DISLOCATION MECHANICS DESCRIPTION OF PLASTIC ANISOTROPY AND FRACTURING OBSERVATIONS IN TEXTURED Al-Li 2090-T8E41 ALLOY

R. W. Armstrong¹ and S. Javadpour²

1. Department of Mechanical Engineering, University of Maryland, College Park, MD 20742, USA

2. Department of Materials and Nuclear Engineering, University of Maryland, College Park, MD 20742, USA

Abstract

Grain boundary strengthening and crystallographic texture influences are being investigated to obtain a better understanding of the anisotropic plastic deformation and cracking behavior exhibited by Al-Li 2090-T8E41 and related alloys. That certain grain boundaries are relatively strong barriers to dislocation slip penetrations is evidenced by boundary protrusions at the circumferential edges of Rockwell B indentations. Nearly parallel slip band traces across apparently aligned grains do not match at grain boundaries. Grain volume cross-slip observations have been made. SEM stereo-pair measurements of fracture facet orientations in fatigue-tested compact tensile specimens are compared with previous measurements and with ideal Cu and brass texture predictions. The conclusion is that the particular fracturing behavior of this alloy is explained by dislocation pile-up induced cracking, enhanced by a favorable dislocation reaction and the presence of grain boundary precipitates, that occur at Cu texture-associated boundaries between relatively large grains.

Introduction

Hall-Petch grain size strengthening results have been described for polycrystalline aluminum material and some of its alloys (1-3). A recent consideration has been to relate such results to polycrystal texture measurements in order to incorporate grain orientation influences into predictive constitutive equations for both face-centered-cubic and body-centered-cubic plastic deformation behaviors (4). For example, the orientation dependence of fundamental Al bicrystal experiments reported in pioneering experiments by Clark and Chalmers (5) have been interpreted on a stereographic projection basis (6) as shown in Figure 1. The experiment was designed to involve the same primary (111) slip plane in both bicrystal halves for various tensile axis (TA) locations rotated about the coincident [111] slip plane normal, that is referenced in the Figure to the initial single crystal 0.5 Schmid factor position on the equatorial bicrystal boundary orientation. Because of slip being initiated independently on different parallel (111) slip planes on either side of the boundary, dislocation pile-ups must form and generate requisite stresses to produce cross-slip at the bicrystal boundary. The $[\bar{1}\bar{1}\bar{1}]$ cross-slip plane normal is shown at

various TA rotations at the bottom of the projection. Even with cross-slip occurring, there is a displacement discontinuity at the boundaries parallel to $[21\bar{1}]$ that builds up with amount of slip forced through the boundaries. A complication for the experiment was that a half-angle rotation just greater than 15° produced double slip for one of the bicrystal halves, as shown below the equator in Figure 1.

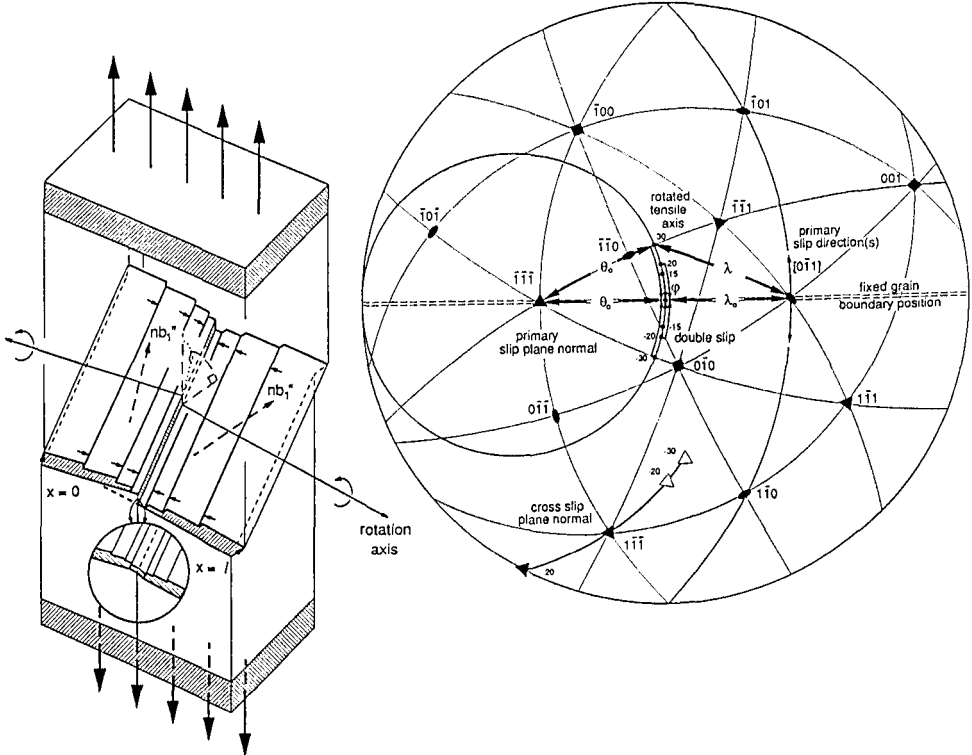


Figure 1. Dislocation mechanics description of pile-ups and stereographic projection analysis for slip processes in pioneering aluminium bicrystal experiments of Clark and Chalmers (5).

Polycrystal Al-Li alloys provide an interesting case of rather well-defined crystallographic slip cutting through precipitate particles within the grains so as to provide for slip band stress concentrations at grain boundaries. From fracture mechanics tests, evidence has been obtained of grain boundary delaminations and slip band cracking attributed to the texture-related anisotropy of slip deformations (7-9). Al-Li alloys might be thought to be favorable to grain size strengthening because of this system possibly being analogous to the Al-Mg system where such Hall-Petch strengthening is known to be important (1,3). In fact, a Hall-Petch microstructural stress intensity of $k = 3.3 \text{ MPa}\cdot[\text{sq rt mm}]$ has been quoted from Al-3Li yield strength results of Jensrud and an upper limit of $k = 6.0 \text{ MPa}\cdot[\text{sq rt mm}]$ was estimated for an Al-2.34Li-1.07Zr alloy with grain boundary precipitate-free zones (10). These k values compare with a lower limiting value of $1.3 \text{ MPa}\cdot[\text{sq rt mm}]$ for Al (11) and an upper limiting value of $8.3 \text{ MPa}\cdot[\text{sq rt mm}]$ from the results of Phillips, Swain and Eborall for an Al-3.5Mg alloy (1).

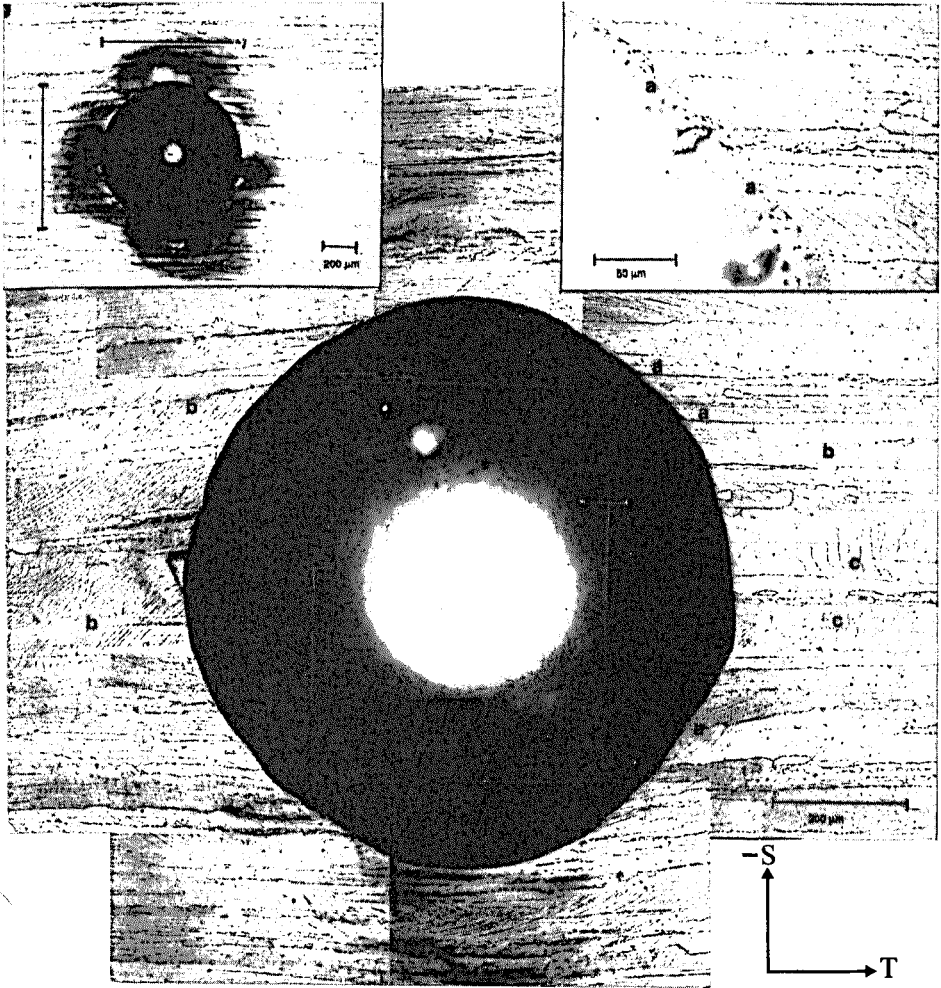


Figure 2. Macroscopic and microscopic plastic anisotropy at a Rockwell B indentation on a previously etched Al-Li 2090-T8E41 L-plane surface.

An indication is shown in the several views of Figure 2 of the slip anisotropy around a Rockwell B indentation put into the L-plane surface of the 2090 alloy material investigated by Yoder et al. (7,8). The residual indentation is ellipsoidal with the major axis along the S (short transverse) direction and minor axis along the T (long transverse) direction (see Yoder et al. reference 7). The top left inset, at relatively low magnification, exhibits shadowing because of the surface relief surrounding the indentation. On a weakest link basis, one might expect that

the material would be "softer" along S. The top right inset shows protrusions of certain boundaries (marked with the letter a) into the indentation cavity in accordance with resistance of the grain boundary regions to deformation. Additional marks are shown in the larger view: at b, for apparent slip band crossings that are revealed at greater magnification not to match at the boundaries; and, at c, for cross-slip observations within the grain volumes to show that though reportedly difficult, cross-slip is able to occur.

Such results as in Figure 2 have been determined for indentations put into the T-plane surface also as an aid to deciphering the texture-sensitive results reported for fracture toughness and fatigue crack growth measurements of the 2090 material (7-9). Additional measurements have been made of the fracture surface morphologies on specimens supplied from the fatigue crack growth tests (7,8). For example, Figure 3 shows, on a combined ideal Cu and brass texture basis, measurements made of the orientations of relatively large, cleavage-like, facets observed on the failure surface of the fatigue-failed material. The method of determining facet plane orientations from SEM stereo-pair measurements has been described by Zhang et al. (12). The (black square) data, above and below the equator, near the vertical axis in the Figure are in agreement with results reported by Yoder et al. In addition, the two measurement points on the equator apply for boundary delaminations. Such delaminations are clearly visible in fracture toughness fractographs presented by Venkateswara et al. (9).

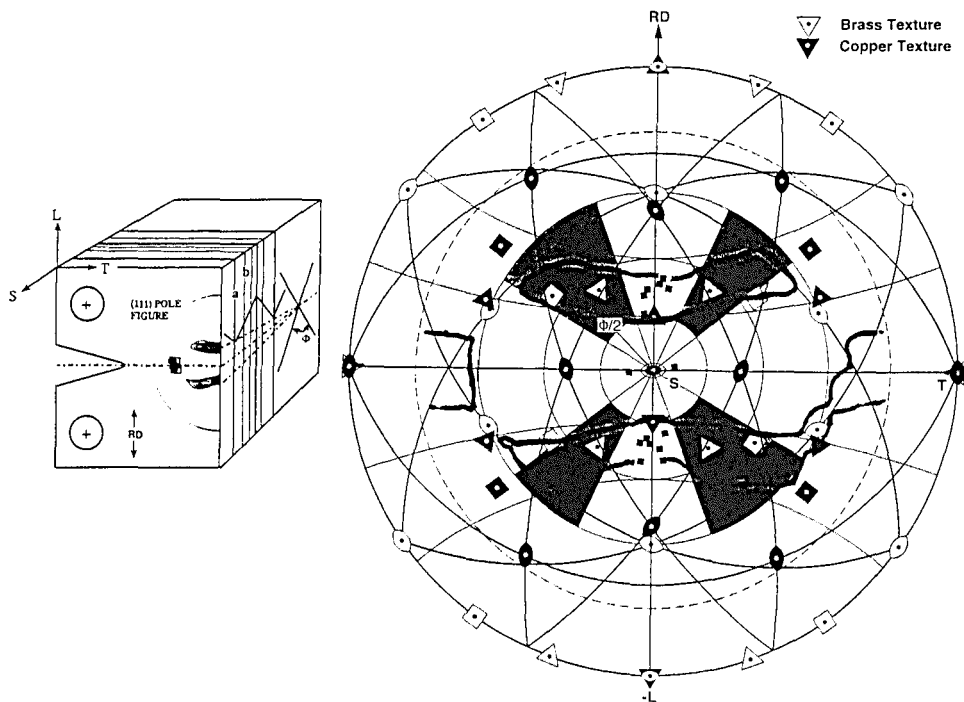


Figure 3. Fracture facet measurements on a combined S-plane stereographic projection showing ideal Cu and brass textures and, also, with experimental $\{111\}$ pole figure results (7).

During the course of metallographic examination of the specimens, it became apparent that precipitation occurred frequently at grain boundaries. Figure 4a,b provides examples of the precipitate structures in the L-plane surface: a, before indentation straining; and, b, in the indentation strain field. Very recently, attention has been directed to the importance of such precipitate particles on limiting the toughness properties of a variety of Al-Li alloys (13). In the case considered here, concern occurs for grain boundary delamination or grain boundary initiated $\{111\}$ cleavage-type fracturing occurring at lesser dislocation pile-up stresses than would be required in the absence of boundary precipitation. Preliminary observations have been made at high optical magnifications of cracking at plate-like boundary precipitates (14).

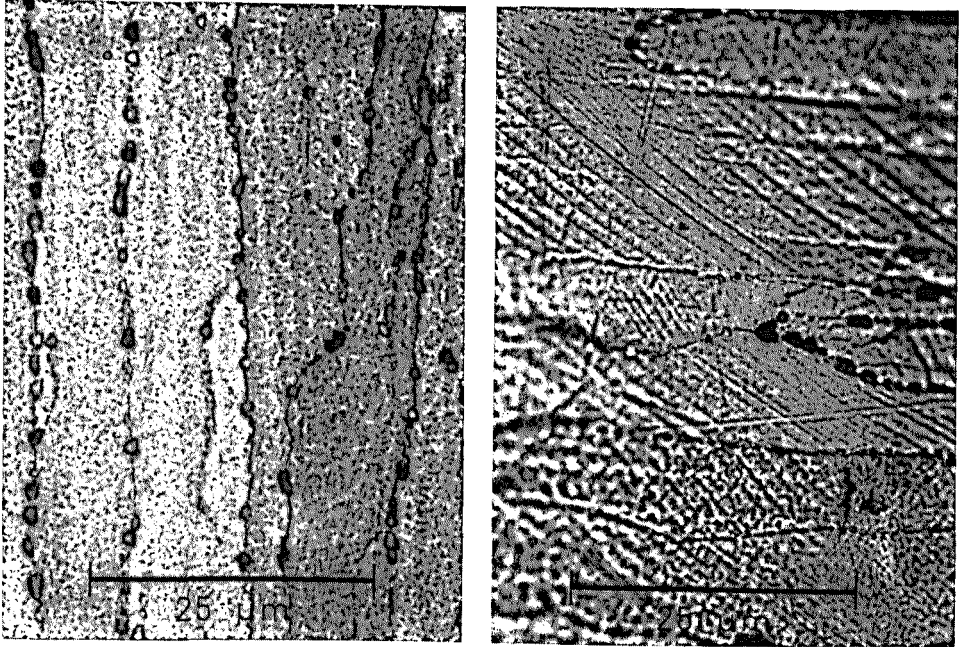


Figure 4. Etched precipitate structures on L-plane surface of Al-Li 2090-T8E41 alloy at grain boundaries: a, before indentation straining; and, b, in the indentation strain field.

Dislocation mechanics/model considerations

As reported by Yoder and colleagues (7,8), the cleavage-like slip plane fracture surfaces identified in Figure 3 are oriented relatively closer to an ideal Cu texture than to the case for the overall stronger brass-type texture that is exhibited by the alloy, consonant with cross-slip supposedly being relatively difficult in 2090 alloy. Thus, the largest crack facets are on $\{111\}$ slip planes having a common T-direction or ideal $\langle 110 \rangle$ rotation axis, making crack growth symmetrical about the T-axis. Such grain orientations should be favorably disposed for crack growth under the applied stress system for the test specimen geometry shown in Figure 3.

To obtain further information about the influence on fracturing behavior of the Cu versus brass components of the textured 2090 alloy, measurements were made of the slip band traces around the Rockwell B indentation on the L-plane surface. Figure 5 shows the results superposed on a stereographic projection containing both ideal texture descriptions. Also, the relative shape of the ellipsoidal indentation is shown at the center of the projection. As indicated, different groupings of the traces were measured for either large or small grains. Slip traces in the small grains were closely aligned around the predicted brass orientations. A number of the traces in the larger grains fit the ideal Cu texture prediction, as indicated by the shaded groupings, however the slip traces in the larger grains are more widely spread. The observations in Figure 5 suggest the possibility that the larger grains exhibit a Cu texture and favor cracking.

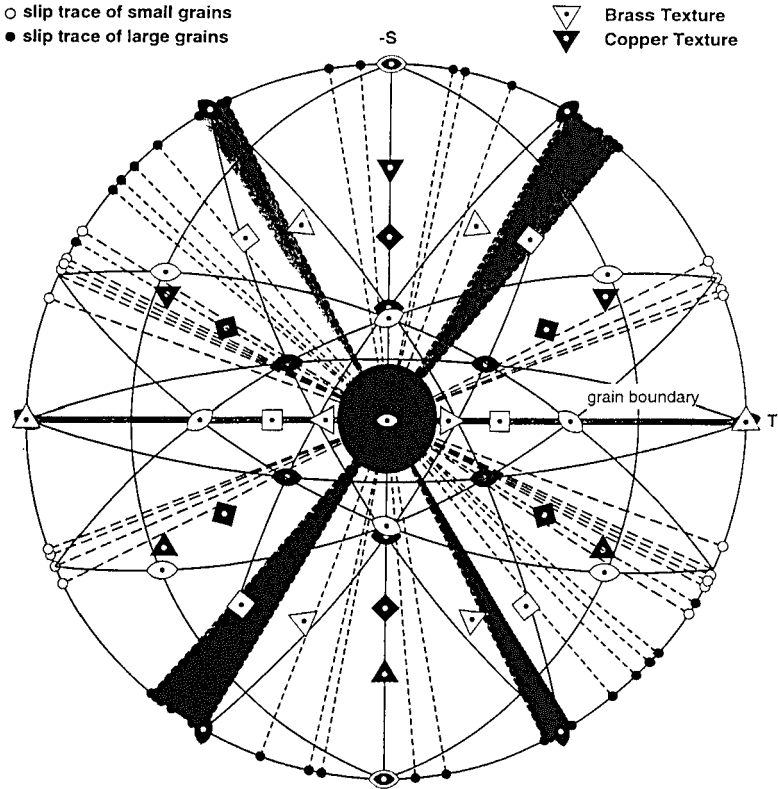


Figure 5. L-plane slip band trace measurements relative to ideal Cu or brass texture predictions for 2090-T8E41 alloy.

The geometrical relationship of slip planes are shown in the T-plane stereographic projection of Figure 6 for an ideal Cu texture orientation stretched along the vertical L (rolling) direction axis; see Figure 3. Figure 6 is a further application of the dislocation mechanics description given for grain boundary reactions of dislocations in directionally-solidified ordered intermetallic alloys (15). In the Figure, the two $\{111\}$ plane poles close to the observed slip systems are on the circumference of the projection. The pair of planes are heavily outlined for activation by the $[11\bar{1}]$ tensile axis, for example, of the $[110]$ slip direction in the $(\bar{1}11)$ slip plane of the left side

Acknowledgements

The 2090 alloy material was provided by A.P. Divecha, Naval Surface Warfare Center, Silver Spring, MD 20910. The fatigue crack growth specimen was supplied by G.R. Yoder, Office of Naval Research (ONR), Arlington, VA 22217. The research has been performed on ONR Contract N00014-90-J-1388.

References

1. R.W. Armstrong, I. Codd, R.M. Douthwaite and N.J. Petch, *Philos. Mag.*, 7, (1962), 45.
2. R.W. Armstrong, *Physics of Materials: Walter Boas Festschrift* (Netley, S.A., Australia: Griffin Press, 1979) 1.
3. J.T. Al-Haidary, N.J. Petch and E.R. de los Rios, *Philos. Mag.*, 47, (1983), 869.
4. F.J. Zerilli and R.W. Armstrong, *J. Appl. Phys.*, 61, (1987), 1816.
5. R. Clark and B. Chalmers, *Acta Metall.*, 2, (1954), 80.
6. R.W. Armstrong, H. Farhangi and V. Ramachandran, "Dislocation Pile-Ups and Deformation Textures" (Univ. Maryland Report presented at The Institute of Metals Meeting; Microstructure and Mechanical Processing, Univ. Cambridge, U.K., 1990).
7. G.R. Yoder, P.S. Pao, M.A. Imam and L.A. Cooley, *Scr. Metall.*, 22, (1988), 1241.
8. P.S. Pao, L.A. Cooley, M.A. Imam and G.R. Yoder, *Scr. Metall.*, 23, (1989), 1455.
9. K.T. Venkateswara Rao, Weikang Yu and R.O. Ritchie, *Metall. Trans.*, 20A, (1989), 485.
10. F.W. Gayle, J.B. VanderSande and O.R. Singleton, *Aluminum Alloys: Their Physical and Mechanical Properties*, Vol. II, ed. E.A. Starke, Jr. and T.H. Sanders, Jr., (Warley, West Midlands, U.K., EMAS Ltd., 1986) 767.
11. N. Hansen, *Acta Metall.*, 25, (1977), 863.
12. X.J. Zhang, A. Kumar, R.W. Armstrong and G.R. Irwin, *Quantitative Methods in Stereology*, (Phila., PA, ASTM STP 1085, 1990) 89.
13. D. Webster, *Adv. Mater. Processes*, 145, (1994) 18.
14. S. Javadpour, "Study of Plastic Anisotropy and Fracturing Observations in Textured Al-Li 2090-T8E41 Alloy", Ph.D. Thesis research in progress, University of Maryland (1994).
15. R.W. Armstrong, *The Yield, Flow and Fracture of Polycrystals*, ed. T.N. Baker, (Barking, U.K., Applied Science Publishers, 1983) 1.